© IWA Publishing 2020
1158

Water Practice & Technology Vol 15 No 4
doi: 10.2166/wpt.2020.089

Removal of dissolved organic nitrogen amino acid from aqueous solutions using activated carbon based on date pits

Badreddine Belhamdi[a,b,*], Zoulikha Merzougui[b], Hamza Laksaci[b], Chemseddine Belabed[c], Salim Boudiaf[d] and Mohamed Trari[e]

[a] Department of Material Sciences, Faculty of Sciences, University of Algiers, 1 Benyoucef Benkhedda, 16002, Algiers, Algeria

[b] Laboratory of Physical and Chemical Study of Materials and Applications in the Environment, Faculty of Chemistry (USTHB), BP 32-16111 EL-Alia, Bab Ezzouar, Algeria

[c] Laboratory of Material Physics, Faculty of Physics, U.S.T.H.B., BP 32 El-Alia, 16111, Algiers, Algeria

[d] Laboratory of Reaction Engineering, Faculty of Mechanical Engineering and Process Engineering, USTHB, BP 32, Algiers, Algeria

[e] Laboratory of Functional Organic Analysis, Faculty of Chemistry (USTHB), BP 32-16111 EL-Alia, Bab Ezzouar, Algeria

*Corresponding author. E-mail: badropg@gmail.com

Abstract

Nitrogenous disinfection by-products (N-DBPs) in chlorinated drinking water are receiving increasing attention due to their elevated toxicities. An effective strategy to control N-DBP formation is to reduce their nitrogenous precursors (amino acids) before disinfection. This work was undertaken to study free amino acid l-tyrosine adsorption onto two activated carbons synthesized from date pits. The amino acid is plentiful in low-molecular weight algal organic matter, which helps the formation of nitrogenous and carbonaceous disinfection by-products during water treatment. The equilibrium adsorption of l-tyrosine was studied on well-characterized activated carbons prepared by KOH (ACK) and $ZnCl_2$ (ACZ) activation, possessing textural properties evaluated by SEM analysis, N_2 adsorption–desorption isotherms and FT-IR spectroscopy. Batch experiments were conducted to determine the activated carbons' adsorption capacities. The effect of contact time, initial adsorbate concentration, solution pH, and temperature were studied. The Langmuir model gave the best fit for the experimental data of l-tyrosine with a maximum monolayer adsorption capacity of 178.57 and 102.04 $mg{\cdot}g^{-1}$ on ACK and ACZ, respectively. Thermodynamic parameters $\Delta G°$, $\Delta H°$ and $\Delta S°$ were also estimated for the adsorption study. The adsorption was spontaneous and exothermic, and involved physisorption.

Key words: activated carbon, date pits, disinfection byproducts, l-tyrosine, physisorption

Highlights

- Date pits are a low-cost precursor for activated carbons.
- The effect of operational parameters on the l-tyrosine removal is optimized.
- The adsorption of l-tyrosine onto ACK and ACZ is favored at pH 6.
- The adsorption kinetic data are well described by a pseudo-first-order model.
- A remarkable activated carbon capacity (178.57 $mg{\cdot}g^{-1}$) is obtained for ACK.

Water Practice & Technology Vol 15 No 4
doi: 10.2166/wpt.2020.089

Graphical Abstract

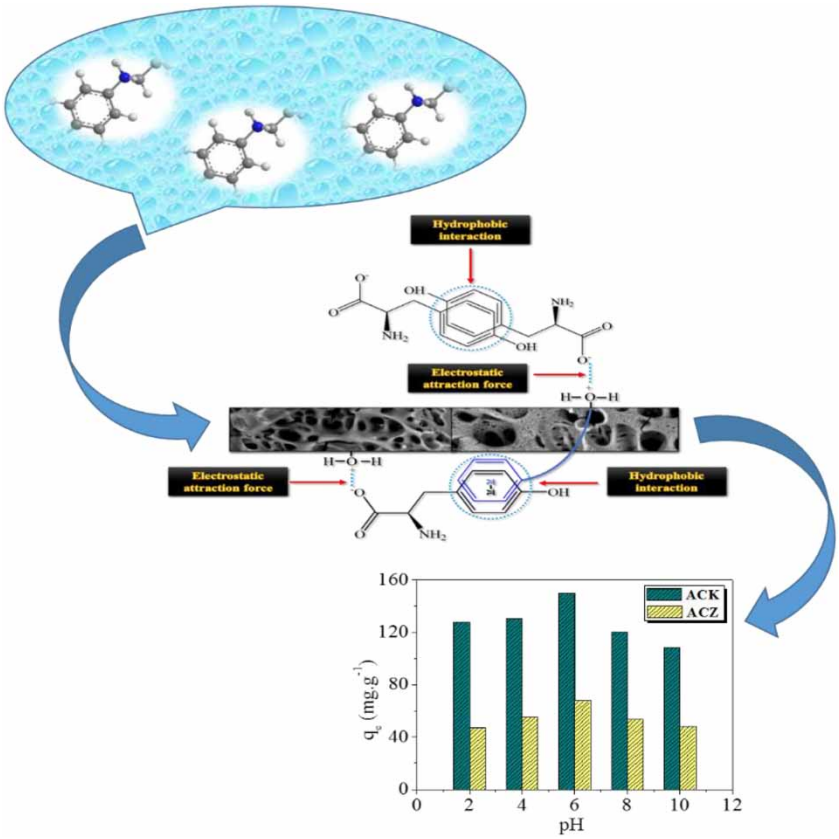

INTRODUCTION

Disinfection, an integral part of water treatment, is carried out daily on large volumes of water worldwide, treating both drinking and, increasingly, recycled waters for use in agriculture, etc (Vo *et al.* 2014; Feng *et al.* 2019). Chemical disinfection may result in the unintended production of disinfectant by-products (DBPs) due to reactions between disinfectants and natural organic matter present in the water. DBPs can be associated with adverse human health effects, including bladder and rectal cancers, and unfavorable pregnancy outcomes (Li & Mitch 2018; Zhang *et al.* 2019). Amino acids (AAs), which are used in various industrial fields, are important precursors for halogenated nitrogenous disinfection by-products (N-DBPs) (Shim *et al.* 2008; Bond *et al.* 2012). These compounds are widely detected in soil, and surface- and ground-water (Thurman 2012). AAs are also precursors for carbonaceous disinfection by-products (C-DBPs), including halo-acetic acids (HAAs) and trihalomethanes (THMs) (Fang *et al.* 2010; Sharma *et al.* 2014).

Chlorinating water containing tyrosine, tryptophan, phenylalanine, asparagine, aspartic acid, histidine and glutamine is reported to lead to the formation of N-DBPs such as haloacetonitriles (HANs) and haloacetamides (HAMs) (Chu *et al.* 2012). HANs and HAMs, commonly detected in chlorinated drinking water, are of growing concern due to their higher cyto- and geno-toxicities in mammalian cell assays than the currently regulated C-DBPs (Muellner *et al.* 2007; Plewa *et al.* 2008). As a result, the occurrence of AAs, including tyrosine, in water could lead to the production of unregulated disinfection by-products, which may have adverse effects on human health. Thus it is necessary to remove tyrosine from water, and find rapid techniques and effective adsorbents for the purpose.

Water Practice & Technology Vol 15 No 4
doi: 10.2166/wpt.2020.089

An effective strategy for controlling DBP formation is to remove their precursors before chlorination. Several effective amino acid removal techniques have been applied in water treatment including nanofiltration over polyelectrolyte membranes (Hong & Bruening 2006), electrodialysis (Readi *et al.* 2013), combined techniques (flotation complexation extraction) (Bi *et al.* 2008), manganese oxide oxidation (Casbeer *et al.* 2013) and adsorption using ionic liquids (Jonckheere *et al.* 2017). Among these, adsorption by activated carbon (AC) has become one of the most reliable methods used (Clark *et al.* 2012). The ability to use ACs as amino acid adsorbents is due to their versatility, which results from their high specific surface, porous structure, high adsorption capacity, and surface chemistry (Kopecka *et al.* 2014; Laksaci *et al.* 2017). Fruit stones – pits – are appropriate raw materials for AC production, as they can be modified by physical and/or chemical treatments to enhance adsorption. Date pits, as an abundant by-product of dates, bring the issue of sustainable use to the preparation of low-cost ACs (Belhamdi *et al.* 2016).

As far as can be ascertained, l-tyrosine removal using date pit-based ACs for water treatment is not yet reported in the literature. This study focuses on the use of granular activated carbons (GACs) to adsorb free amino acids during water chlorination. The main objective was to evaluate the adsorption capacities of ACs prepared from date pits by chemical activation with KOH and $ZnCl_2$ ACK and ACZ respectively, for l-tyrosine removal under various conditions – that is, initial concentration, contact time, solution pH and temperature.

MATERIALS AND METHODS

Adsorbate

The free amino acid (l-tyrosine) used came from Sigma Aldrich (Figure 1). It has been identified in natural waters at higher concentrations than many other free amino acids (Fang *et al.* 2010).

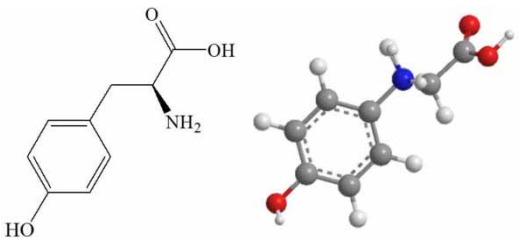

Figure 1 | Molecular structure of l-tyrosine amino acid.

Preparation and characterization of ACs

Two activated carbons were used as low-cost adsorbents to remove l-tyrosine from aqueous solution. Both are microporous and designed for water treatment based on the results of previous studies, including adsorption of low molecular weight natural organic matter (l-phenylalanine amino acid), and taste and odor compounds (Belhamdi *et al.* 2016). The activated carbons were synthetized from date pits using KOH and $ZnCl_2$ as activating agents. The raw material was first washed repeatedly with distilled water, and then dried at 120 °C. The samples were crushed and sieved into uniform size ranging from 0.5 to 1 mm. The dried precursor was impregnated with a chemical activating agent in solid form (1 g $ZnCl_2$: 1 g date pits) and (9 mmol KOH: 1 g date pits). These mixtures were heated in a tubular furnace at 600 and 800 °C, respectively, for 1 hour under nitrogen flow, a heating rate of 5 °C·min^{-1}. After cooling at room temperature, the activated products were washed with HCl (0.1 M)

Water Practice & Technology Vol 15 No 4
doi: 10.2166/wpt.2020.089

and hot distilled water until the wash-water test with $AgNO_3$ was negative, and then dried at 120 °C. The resulting activated carbons are denoted ACZ ($ZnCl_2$) and ACK (KOH).

The textural properties of ACK and ACZ are given in Table 1 and Figure 2.

Table 1 | Textural characteristics of ACK and ACZ

	Specific surface ($m^2 \cdot g^{-1}$)			Pore volume ($cm^3 \cdot g^{-1}$)			
Adsorbent	S_{BET}	S_{ext}	S_{mic}	V_T	V_{mes}	V_{mic}	**DFT pore size (nm)**
ACK	1,209	276	933	0.550	0.180	0.370	1.48
ACZ	1,235	525	710	0.630	0.341	0.289	1.59

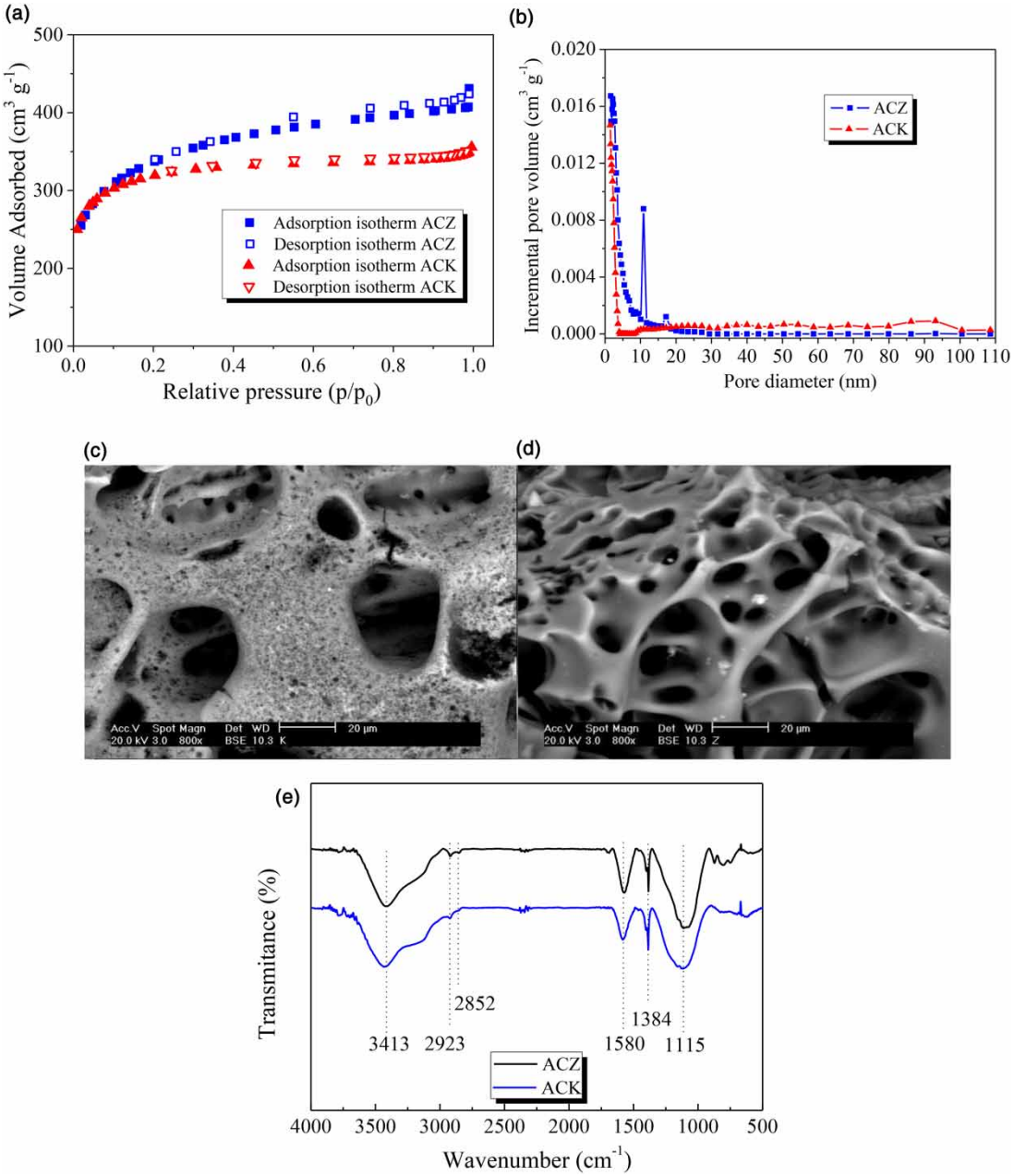

Figure 2 | (a) Nitrogen adsorption-desorption isotherms of ACK and ACZ at –77 K; (b) DFT pore size distribution for ACK and ACZ; (c) SEM image of ACK; (d) SEM image of ACZ; (e) FTIR spectra of ACK and ACZ.

Water Practice & Technology Vol 15 No 4
doi: 10.2166/wpt.2020.089

Adsorption experiments

Kinetic studies

In the l-tyrosine kinetic studies for ACK and ACZ, batch experiments were carried out at ambient temperature and a mixing speed of 150 rpm. The effect of contact time was investigated in the range 5–360 minutes. The initial l-tyrosine concentrations used were 60, 100 and 200 mg·L^{-1}, and volume, temperature and solution pH were 50 mL, 293 K and natural pH, respectively. After each batch test, the supernatant solution was filtered with a hydrophilic syringe filter to enable determination of the residual concentrations of l-tyrosine. The amount adsorbed was determined using a UV-Vis spectrophotometer at 275 nm. The adsorbents' adsorption capacity per unit mass q_e (mg·g^{-1}) and adsorption ratio E (%) were calculated using Equations (1) and (2):

$$q_e = \frac{(C_0 - C_e)V}{W} \tag{1}$$

$$E(\%) = \frac{C_0 - C_e}{C_0} \times 100 \tag{2}$$

where C_o and C_e are the initial and equilibrium concentrations of l-tyrosine in liquid phase, respectively (mg·L^{-1}); V (L) the volume of solution and W (g) the dried mass of carbon sample.

The data from the kinetic curves were analyzed with pseudo-first order, pseudo-second order (Konggidinata *et al.* 2017; Ahmad *et al.* 2018) and intra-particle diffusion (Weber & Morris 1965) kinetic models – Equations (3)–(5).

$$\ln(q_e - q_t) = \ln q_e - k_1 t \tag{3}$$

$$\frac{t}{q_t} = \frac{1}{k_2 q_e^2} + \frac{t}{q_e} \tag{4}$$

$$q_t = k_p t^{1/2} + C \tag{5}$$

where q_t and q_e (both mg·g^{-1}) are the amounts of l-tyrosine adsorbed at time t (min) and equilibrium, respectively; k_1 (min^{-1}) and k_2 (g·mg^{-1}·min^{-1}) the adsorption rate constants of the pseudo-first and pseudo-second order models, respectively; k_p (mg·g^{-1}·$min^{-1/2}$) is the intra-particle diffusion rate constant and C the intercept associated with the boundary layer thickness, given by the slope and intercept of the straight line respectively. If the plot q_t versus $t^{1/2}$ passes through the origin, then intra-particle diffusion is the rate-limiting step (Drweesh *et al.* 2016).

Effect of solution pH

A standard adsorbent dose (50 mg) was added in 100 mL flasks containing 50 mL of l-tyrosine solution (200 mg L^{-1}) at different pH values. The solution pH was adjusted by adding NaOH or HCl (0.1 M) to achieve pH values between 2 and 10, and the reaction mixture agitated on a water bath shaker at 293 K for 360 min, a time interval pre-determined as sufficient for adsorption equilibrium to be reached. The l-tyrosine uptake, q_e (mg·g^{-1}), was calculated using Equation (1).

Equilibrium adsorption isotherm

The l-tyrosine aqueous solution adsorption isotherms were measured using a static method. 50 mg of each AC was added to 50 mL of l-tyrosine solution at different initial concentrations from 20 to 240 mg·L^{-1}. The flasks were covered and stirred at 150 rpm for 360 min at 293 K, before the solution

Water Practice & Technology Vol 15 No 4
doi: 10.2166/wpt.2020.089

was filtered and analyzed using a UV–visible spectrophotometer (JASCO V-630) at 275 nm. The amount adsorbed q_e ($mg{\cdot}g^{-1}$) was calculated using Equation (1).

Adsorption isotherms are used to describe adsorbate/adsorbent interactions. The parameters obtained from different models provide information on the adsorption mechanisms, surface properties and adsorbent affinities. There are several equations for analyzing experimental adsorption equilibrium data and, in this study, the Langmuir, Freundlich and Redlich–Peterson (R–P) isotherm models were used.

The Langmuir model is expressed in Equations (6) and (7) (Langmuir 1918; Konggidinata *et al.* 2017):

$$q_e = \frac{q_{max}.\ K_L.\ C_e}{1\ +\ K_L.\ C_e} \tag{6}$$

$$\frac{C_e}{q_e} = \frac{1}{q_{max}K_L} + \frac{C_e}{q_{max}} \tag{7}$$

where K_L ($L{\cdot}mg^{-1}$) is the Langmuir constant related to the maximum adsorption capacity and energy of sorption; and q_e and q_{max} the equilibrium and maximum adsorption capacities ($mg{\cdot}g^{-1}$), respectively.

Another important parameter, R_L, the separation factor, is the essential characteristic of the Langmuir isotherm and is defined by Equation (8):

$$R_L = \frac{1}{1\ +\ K_L C_0} \tag{8}$$

where C_o ($mg{\cdot}L^{-1}$) is the highest initial concentration of l-tyrosine and R_L indicates the potential for adsorption:

favorable $(0 < R_L < 1)$;

unfavorable $(R_L > 1)$;

Linear $(R_L = 1)$; or

irreversible $(R_L = 0)$

The Freundlich model is expressed by Equations (9) and (10) (Cazetta *et al.* 2011; Konggidinata *et al.* 2017):

$$q_e = K_F\ .C_e^{1/n} \tag{9}$$

$$\ln q_e = \ln K_F + \frac{1}{n}\ln C_e \tag{10}$$

where K_F is the Freundlich constant and n the heterogeneity factor.

Water Practice & Technology Vol 15 No 4
doi: 10.2166/wpt.2020.089

The nonlinear and linear forms of the R–P isotherm are expressed in Equations (11) and (12), respectively (Wu *et al.* 2010):

$$q_e = \frac{q'_{max} b_{RP} C_e}{1 + b_{RP} C_e} \tag{11}$$

$$\frac{C_e}{q_e} = \frac{1}{b_{RP} q'_{max}} + \left(\frac{1}{q'_{max}}\right) C_e^{\alpha} \tag{12}$$

where b_{RP} and α are R–P constants, and q'_{max} the maximum adsorption capacity ($mg \cdot g^{-1}$).

Thermodynamics parameters

The free energy (ΔG°), enthalpy (ΔH°) and entropy (ΔS°) of l-tyrosine adsorption on ACK and ACZ, are calculated using Equations (13) and (14) to understand the nature of the adsorption (Tran *et al.* 2017). The parameters are determined from the equilibrium constant K_C (q_e/C_e), which depends on the temperature.

$$\Delta G^0 = -RT \ln(\rho K_C) \tag{13}$$

$$\ln(\rho K_C) = \frac{\Delta S^0}{R} - \frac{\Delta H^0}{RT} \tag{14}$$

where R is the gas constant, T the absolute temperature and ρ the density of water ($1{,}000\ g \cdot L^{-1}$). ΔH° and ΔS° are calculated from the slope and intercept of $\ln(\rho K_C)$ vs. 1/T, respectively.

RESULTS AND DISCUSSION

AC adsorption capacities

Adsorption kinetics

The change in the amount of l-tyrosine adsorbed onto ACK and ACZ as a function of contact time is illustrated in Figure 3. Adsorption efficiency increases rapidly at first, then more moderately. The increasing trend stopped when equilibrium was reached, within 240 minutes for each AC. Three l-tyrosine concentrations (60, 100 and 200 $mg \cdot L^{-1}$) were also used to investigate the effect of initial concentration on its adsorption. The adsorption capacity of both ACK and ACZ increases with increasing initial l-tyrosine concentration (Figure 3), reaching experimental values of 154.68 and 68.76 $mg \cdot g^{-1}$, respectively, at 200 $mg \cdot L^{-1}$. ACK has the higher l-tyrosine adsorption capacity due to its relatively larger microporous surface area and high microporous volume (Belhamdi *et al.* 2019). The enhanced adsorption capacity of both ACs at higher initial l-tyrosine concentrations can be explained by an increase in the driving force, due to the concentration gradient with increased initial l-tyrosine concentration, overcoming the mass transfer resistance of l-tyrosine molecules between the aqueous phase and solid surface.

The controlling mechanism of l-tyrosine adsorption by ACK and ACZ was studied by fitting the experimental data with the pseudo- first and second order, and the intra-particle diffusion kinetic models – see Table 2. Although the R^2 values of the pseudo-first order kinetic model are all acceptable (>0.96), the adsorption capacities estimated from experimental data for l-tyrosine do not correlate with that model, which is invalid for testing the l-tyrosine/ACs system. An evaluation of both the

Water Practice & Technology Vol 15 No 4
doi: 10.2166/wpt.2020.089

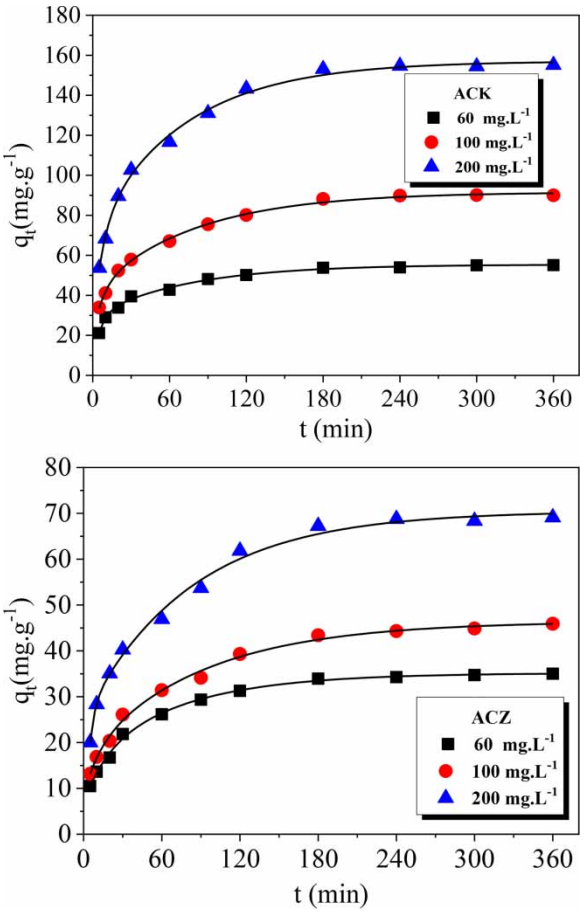

Figure 3 | Effect of contact time on l-tyrosine adsorption onto ACK and ACZ (initial l-tyrosine concentration: 60, 100 and 200 mg·L $^{-1}$; adsorbent dose 1 g·L^{-1}; shaking speed 150 rpm; temperature 293 K).

Table 2 | Parameters of pseudo-first order, pseudo-second order and intra-particle diffusion models for l-tyrosine adsorption onto ACK and ACZ

			Co (mg·L $^{-1}$)		
Adsorbent	**Kinetic model**	**Parameter**	**60**	**100**	**200**
ACK	Pseudo-first order	$q_{e,exp}$ (mg·g^{-1})	53.81	88.20	154.68
		$q_{e,cal}$ (mg·g^{-1})	29.98	53.46	100.41
		k_1 (min^{-1})	0.0179	0.0159	0.0184
		R^2	0.993	0.989	0.979
	Pseudo-second order	$q_{e,cal}$ (mg·g^{-1})	57.14	94.96	162.86
		k_2 (g·mg^{-1}·min^{-1})	0.0013	0.0006	0.0004
		R^2	0.999	0.998	0.998
	Intra-particle diffusion	k_p (mg·g^{-1}·min$^{-1/2}$)	1.87	3.85	4.93
		C_2	29.20	37.50	83.30
		R^2	0.980	0.992	0.904
ACZ	Pseudo-first order	$q_{e,exp}$ (mg·g^{-1})	33.93	43.39	68.76
		$q_{e,cal}$ (mg·g^{-1})	24.10	31.39	48.40
		k_1 (min^{-1})	0.0185	0.0159	0.0166
		R^2	0.993	0.969	0.995
	Pseudo-second order	$q_{e,cal}$ (mg·g^{-1})	37.00	48.78	73.63
		k_2 (g·mg^{-1}·min^{-1})	0.0013	0.0008	0.0006
		R^2	0.999	0.996	0.996
	Intra-particle diffusion	k_p (mg·g^{-1}·min$^{-1/2}$)	1.53	2.21	3.04
		C_2	14.07	14.00	24.65
		R^2	0.981	0.988	0.954

Water Practice & Technology Vol 15 No 4
doi: 10.2166/wpt.2020.089

R^2 coefficients and the estimated q_e ($mg \cdot g^{-1}$) values indicates that l-tyrosine adsorption onto ACK and ACZ is described better by the pseudo-second order model.

Weber and Morris' proposed intra-particle diffusion model (Figure 4) was applied to identify whether intra-particle or film diffusion is the rate-limiting step. As the intra-particle diffusion plot does not pass through the origin, with values of $R^2 > 0.954$ (Table 2), the model suggests that the l-tyrosine adsorption mechanism onto ACK and ACZ is complex and governed by more than one mechanism, and that intra-particle diffusion was not the only rate-limiting stage (Alves *et al.* 2013b). It is assumed that external mass transfer is significant only in the first stage of adsorption.

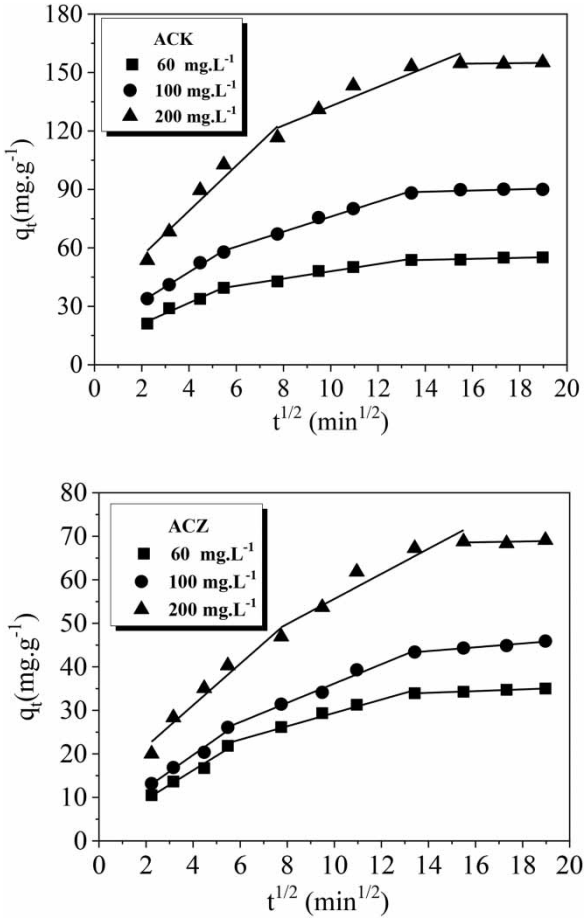

Figure 4 | Intra-particle diffusion for the adsorption of l-tyrosine onto ACK and ACZ.

Effect of pH

The l-tyrosine adsorption by ACK and ACZ is affected strongly by the solution's initial pH (Figure 5). The pH determines species of l-tyrosine in the solution as well as affecting the ACs' surface properties. The pH at the point of zero charge (pH_{PZC}) was respectively 6.18 and 6.80 for ACZ and ACK (Belhamdi *et al.* 2016) – that is, their surfaces have a negative charge when the pH exceeds the pH_{PZC}. Cationic ($^{+}NH_3$–R–COOH), zwitterionic ($^{+}NH_3$–R–COO^{-}), and anionic (NH_2–R–COO^{-}) compounds are formed according to the isoelectric point of l-tyrosine (Tran *et al.* 2018). At pH 2 and 4, the repulsive electrostatic interactions between ACs (strong positive charge) and l-tyrosine protonated amino groups ($^{+}NH_3$-R-COOH) in an acidic medium reduced the adsorption capacity. In contrast, adsorption was enhanced significantly when solution pH increased from 4.0 to 6.0. A possible explanation, based on l-tyrosine's hydrophobicity, is proposed in Figure 6. The higher hydrophobicity of l-tyrosine molecules at pH 6 means that hydrophobic interactions must occur to

Water Practice & Technology Vol 15 No 4
doi: 10.2166/wpt.2020.089

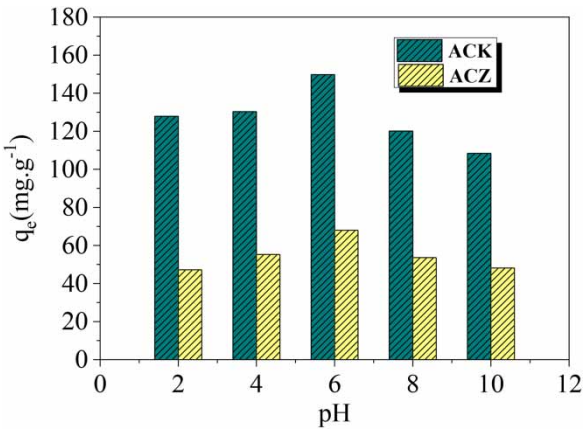

Figure 5 | Effect of pH on l-tyrosine adsorption onto ACK and ACZ (initial l-tyrosine concentration: 200 mg·L $^{-1}$; adsorbent dose 1 g·L^{-1}; shaking speed 150 rpm; temperature 293 K).

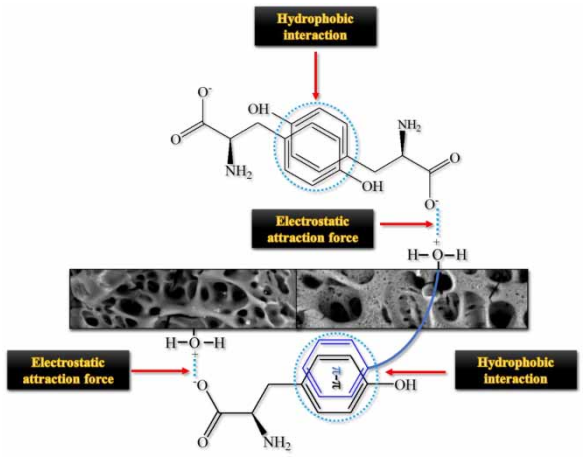

Figure 6 | Schematic illustration of possible interaction forces involved in l-tyrosine adsorption onto the two ACs.

minimize contact with water (Goscianska *et al.* 2014) – the l-tyrosine molecules stand with their hydrophobic elements together to displace water molecules. The carboxylic groups of the l-tyrosine molecules interact strongly with positively charged sites on the ACK and ACZ surface (pH > pH_{PZC}) by electrostatic attraction.

Adsorption capacity fell significantly in basic solutions at pH 8 and 10. The dominant species is (NH_2-R-COO^-, pH > PI 5.66), the surface charge of the two ACs is negative, and the repulsive electrostatic interactions are unfavorable to l-tyrosine adsorption.

Adsorption isotherms

The adsorption isotherms, represented as the amount of l-tyrosine adsorbed onto ACK and ACZ at equilibrium (q_e, mg·g^{-1}) versus the amount of amino acid remaining in solution (C_e, mg·L^{-1}), are shown in Figure 7. The l-tyrosine isotherm is L-shaped (Langmuir) according to the classification by Giles *et al.* (Giles *et al.* 1960), which means that there is limited competition between the solvent and l-tyrosine molecules to occupy ACK and ACZ surface sites. The initial part of the L-curve suggests low interaction between amino acid molecules and AC adsorption sites at low concentrations, while, for high initial concentrations, adsorption occurs more readily. This may be due to l-tyrosine amino acid's non-polar groups getting closer to each other until they are within their van der Waal radii at high concentrations, leading to dense molecular packing on ACs' active sites (Goscianska *et al.*

Water Practice & Technology Vol 15 No 4
doi: 10.2166/wpt.2020.089

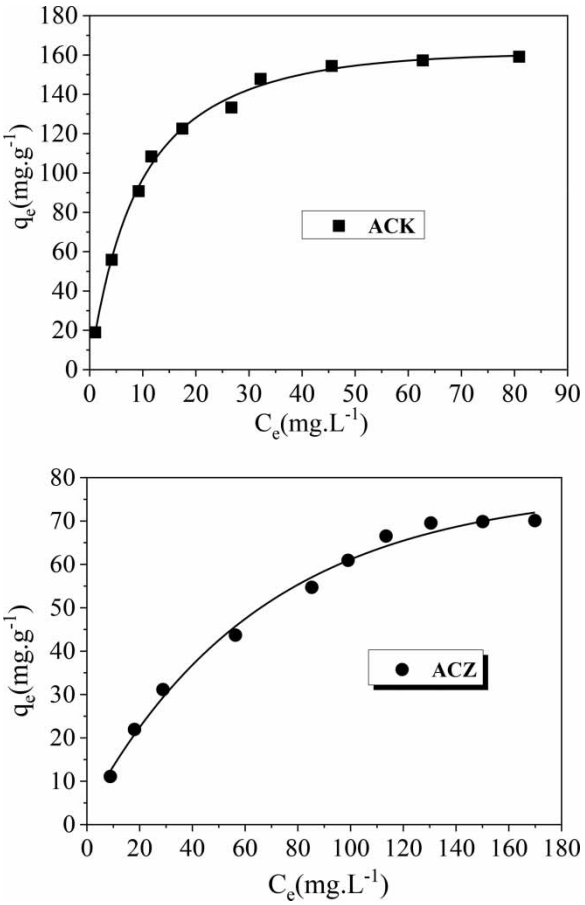

Figure 7 | l-tyrosine adsorption isotherms onto ACK and ACZ (initial concentration: 20–240 mg·L $^{-1}$; adsorbent dose 1 g·L^{-1}; shaking speed 150 rpm; temperature 293 K).

2014). The experimental equilibrium data are described by the Langmuir, Freundlich and R-P models (see section 2.2.2. Equilibrium adsorption isotherm).

The parameters deduced from different isotherm models give information on the adsorption mechanisms, surface properties and l-tyrosine affinity. The model parameters obtained from linear plots are given in Table 3. On the basis of R^2, the equilibrium data for l-tyrosine adsorption onto ACK and ACZ are fitted well by the Langmuir and R-P models. In contrast, the Freundlich isotherm does not provide

Table 3 | Langmuir, Freundlich and Redlich–Peterson constants for l-tyrosine removal by ACK and ACZ

		Adsorbent	
Isotherm model	**Constant**	**ACK**	**ACZ**
Langmuir	q_{max} (mg·g^{-1})	178.57	102.04
	k_L (L·mg^{-1})	0.1222	0.0145
	R^2	0.998	0.989
Freundlich	k_F	26.28	3.44
	n	2.106	1.625
	R^2	0.906	0.974
Redlich–Peterson	q'_{max} (mg·g^{-1})	169.49	94.34
	b_{RP}	0.1319	0.0159
	α	0.991	0.985
	R^2	0.998	0.990

Water Practice & Technology Vol 15 No 4
doi: 10.2166/wpt.2020.089

a good fit – R^2 0.90 and 0.97. It is thought, therefore, that the surfaces of ACK and ACZ display homogeneous adsorption site distribution and monolayer adsorption of l-tyrosine (Konggidinata *et al.* 2017). The maximum monolayer adsorption capacities were found to be 178.57 and 102.04 mg·g^{-1} on ACK and ACZ, respectively at 293 K and pH 6. The heterogeneity factor, n, of the Freundlich model is in the range 1–10, indicating favorable adsorption conditions. Non-linear fitting of the isotherm models was also studied – see Figure 8(a) and 8(b). Both the Langmuir and R-P isotherms can generate satisfactory fits to the l-tyrosine experimental data, unlike the Freundlich model. The

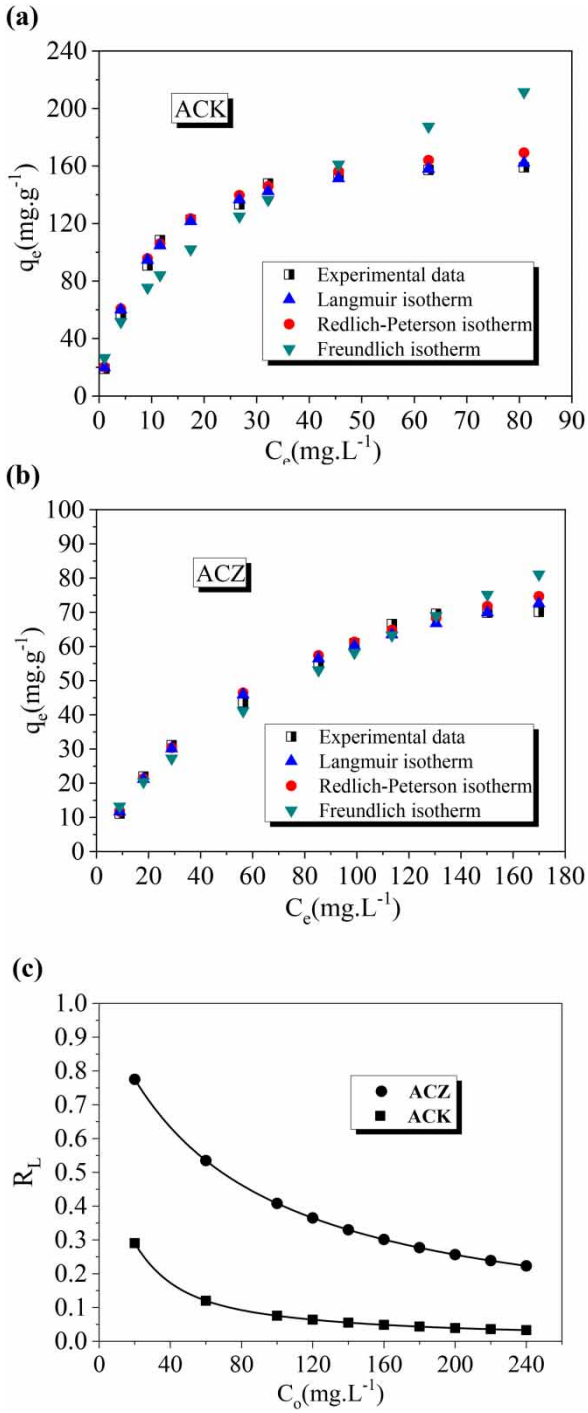

Figure 8 | (a and b) Non-linear plots of Langmuir, Freundlich and R–P models for l-tyrosine adsorption onto ACK and ACZ; (c) effect of l-tyrosine concentration on dimensionless equilibrium parameter R_L.

Water Practice & Technology Vol 15 No 4
doi: 10.2166/wpt.2020.089

calculated R_L values versus the initial l-tyrosine amino acid concentration for the two ACs (Figure 8(c)) are between 0 and 1, indicating that the adsorption process is favorable. This confirms that the Langmuir isotherm is favorable for l-tyrosine adsorption onto ACK and ACZ at 293 K.

Adsorption thermodynamics

The effect of temperature on l-tyrosine adsorption is reported in Figure 9. The quantity adsorbed decreases with increasing temperature – that is, low temperatures favor l-tyrosine removal. This is likely to be due to the tendency of l-tyrosine molecules to form hydrophobic bonds in aqueous solution, hindering their hydrophobic interactions with the AC surface (Alves *et al.* 2013b).

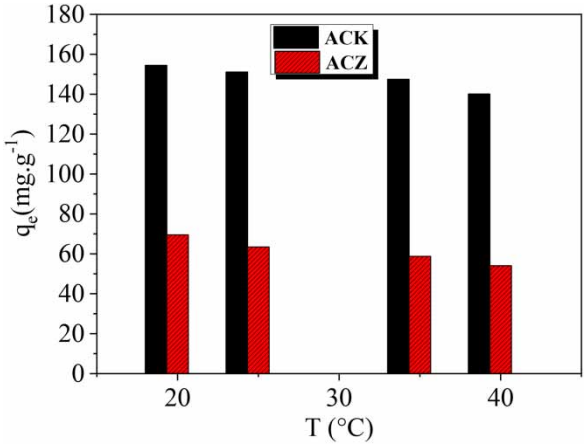

Figure 9 | Effect of temperature on l-tyrosine adsorption onto ACK and ACZ (initial concentration 200 mg·L^{-1}; adsorbent dose 1 g·L^{-1}; shaking speed 150 rpm; temperature 293 K).

The standard free energy (ΔG°), standard enthalpy (ΔH°), and standard entropy (ΔS°), evaluated from Equations (9) and (10), are shown in Table 4 and Figure 10. Negative ΔG° indicates that l-tyrosine removal from water is spontaneous for both ACs. Negative ΔH° confirms that adsorption was exothermic and physical in nature for both ACs. Positive ΔS° indicates that the randomness of the l-tyrosine molecules when in solution increases during their adsorption onto the ACs (Belhamdi *et al.* 2019).

Table 4 | Thermodynamic parameters for l-tyrosine adsorption

Adsorbent	T (K)	K_c	ΔG° (kJ·mol^{-1})	ΔH° (kJ·mol^{-1})	ΔS° (kJ·mol^{-1}·K^{-1})	Van't Hoff equation
ACK	293	3.386	−19.799	−12.721	0.024	$y = 1530.15x + 2.91$
	298	3.078	−19.907			$R^2 = 0.926$
	308	2.805	−20.330			
	313	2.338	−20.187			
ACZ	293	0.519	−15.230	−9.953	0.018	$y = 1197.19x + 2.18$
	293	0.497	−15.386			$R^2 = 0.953$
	293	0.446	−15.622			
	293	0.395	−15.560			

Comparison of results with literature

The efficiency of ACK and ACZ was also compared with results reported from some other studies. Table 5 shows that the adsorption capacity of ACK and ACZ exceeds that of many adsorbents,

Water Practice & Technology Vol 15 No 4
doi: 10.2166/wpt.2020.089

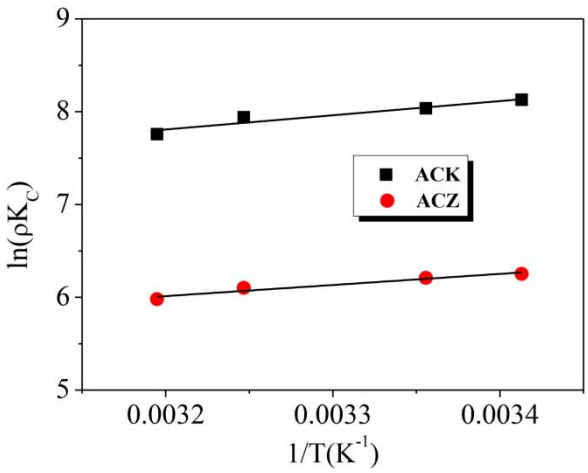

Figure 10 | $\ln pK_C$ vs 1/T for l-tyrosine adsorption onto ACK and ACZ.

Table 5 | Studies of l-tyrosine amino acid removal by various adsorbents

Adsorbent	q_{max}(mg·g^{-1})	Reference
ACK	178.57	This study
ACZ	102.04	This study
Fe_3O_4/SiO_2/CMCD MNPs	5.43	Ghosh *et al.* (2011)
Mg/Al layered double hydroxides	345.00	Tran *et al.* (2018)
AC from corn cobs	14.00	Alves *et al.* (2013a)
NaZSM-5 zeolite	14.86	Titus *et al.* (2003)
β-cyclodextrin polymer	3.20	Tang *et al.* (2006)
Fe_3O_4 magnetic nanoparticles	12.74	Kamran (2016)

suggesting that the two ACs have potential as adsorbents for the removal of dissolved organic nitrogen amino acid in water treatment, especially l-tyrosine.

CONCLUSIONS

In this study the dynamic adsorption of l-tyrosine onto date pit-based ACs was investigated. Removal of this typical amino acid from aqueous solution was controlled by factors affecting adsorption capacity such as contact time, initial l-tyrosine concentration, pH and temperature. Adsorption capacity decreased with temperature and increased with increasing initial l-tyrosine concentration. On the basis of the R^2 values, and the difference between the experimental and calculated values of q_e, the pseudo second-order kinetic model provides a better fit than the pseudo-first-order model for l-tyrosine adsorption by ACK and ACZ. Weber and Morris' proposed intra-particle diffusion model suggested that adsorption in this case is governed by more than one mechanism and that intra-particle diffusion is not the only rate limiting step.

The adsorption system was evaluated using the Langmuir, Freundlich and R–P models. The highest correlation coefficient (R^2) obtained indicated that the adsorption process is best described by the Langmuir and R-P models. The two adsorbents – ACK and ACZ – have monolayer adsorption capacities as 178.57 and 102.04 mg·g^{-1}, respectively under optimized conditions – temperature 293 K, pH 6 and mixing time 360 minutes. The thermodynamic data show that l-tyrosine adsorption onto ACK and ACZ is feasible and is exothermic.

Water Practice & Technology Vol 15 No 4
doi: 10.2166/wpt.2020.089

ACKNOWLEDGEMENTS

The authors wish to express their thanks for financial support from the Faculty of Chemistry (USTHB, Algiers), and for the Directorate General of Scientific Research and Technological Development (DGSRTD, Algiers).

DATA AVAILABILITY STATEMENT

All relevant data are included in the paper or its Supplementary Information.

REFERENCES

Ahmad, Z. U., Lian, Q., Zappi, M. E., Buchireddy, P. R. & Gang, D. D. 2018 Adsorptive removal of resorcinol on a novel ordered mesoporous carbon (OMC) employing COK-19 silica scaffold: kinetics and equilibrium study. *Journal of Environmental Sciences* **75**, 307–317.

Alves, C. C., Franca, A. S. & Oliveira, L. S. 2013a Evaluation of an adsorbent based on agricultural waste (corn cobs) for removal of tyrosine and phenylalanine from aqueous solutions. *Biomed Research International* **2013**, 978256.

Alves, C. C. O., Franca, A. S. & Oliveira, L. S. 2013b Removal of phenylalanine from aqueous solutions with thermo-chemically modified corn cobs as adsorbents. *LWT – Food Science and Technology* **51**(1), 1–8.

Belhamdi, B., Merzougui, Z., Trari, M. & Addoun, A. 2016 A kinetic, equilibrium and thermodynamic study of l-phenylalanine adsorption using activated carbon based on agricultural waste (date stones). *Journal of Applied Research and Technology* **14**(5), 354–366.

Belhamdi, B., Merzougui, Z., Laksaci, H. & Trari, M. 2019 The removal and adsorption mechanisms of free amino acid l-tryptophan from aqueous solution by biomass-based activated carbon by H_3PO_4 activation: regeneration study. *Physics and Chemistry of the Earth, Parts A/B/C* **114**, 102791.

Bi, P., Dong, H., Yu, H. & Chang, L. 2008 A new technique for separation and purification of l-phenylalanine from fermentation liquid: flotation complexation extraction. *Separation and Purification Technology* **63**(2), 487–491.

Bond, T., Templeton, M. R. & Graham, N. 2012 Precursors of nitrogenous disinfection by-products in drinking water-–a critical review and analysis. *Journal of Hazardous Materials* **235**, 1–16.

Casbeer, E. M., Sharma, V. K., Zajickova, Z. & Dionysiou, D. D. 2013 Kinetics and mechanism of oxidation of tryptophan by ferrate (VI). *Environmental Science & Technology* **47**(9), 4572–4580.

Cazetta, A. L., Vargas, A. M., Nogami, E. M., Kunita, M. H., Guilherme, M. R., Martins, A. C., Silva, T. L., Moraes, J. C. & Almeida, V. C. 2011 NaOH-activated carbon of high surface area produced from coconut shell: kinetics and equilibrium studies from the methylene blue adsorption. *Chemical Engineering Journal* **174**(1), 117–125.

Chu, W., Gao, N., Yin, D., Deng, Y. & Templeton, M. R. 2012 Ozone–biological activated carbon integrated treatment for removal of precursors of halogenated nitrogenous disinfection by-products. *Chemosphere* **86**(11), 1087–1091.

Clark, H. M., Alves, C. C. C., Franca, A. S. & Oliveira, L. S. 2012 Evaluation of the performance of an agricultural residue-based activated carbon aiming at removal of phenylalanine from aqueous solutions. *LWT – Food Science and Technology* **49**(1), 155–161.

Drweesh, S. A., Fathy, N. A., Wahba, M. A., Hanna, A. A., Akarish, A. I., Elzahany, E. A., El-Sherif, I. Y. & Abou-El-Sherbini, K. S. 2016 Equilibrium, kinetic and thermodynamic studies of Pb (II) adsorption from aqueous solutions on HCl-treated Egyptian kaolin. *Journal of Environmental Chemical Engineering* **4**(2), 1674–1684.

Fang, J., Yang, X., Ma, J., Shang, C. & Zhao, Q. 2010 Characterization of algal organic matter and formation of DBPs from chlor(am)ination. *Water Research* **44**(20), 5897–5906.

Feng, H., Ruan, Y., Wu, R., Zhang, H. & Lam, P. K. 2019 Occurrence of disinfection by-products in sewage treatment plants and the marine environment in Hong Kong. *Ecotoxicology and Environment Safety* **181**, 404–411.

Ghosh, S., Badruddoza, A. Z. M., Uddin, M. S. & Hidajat, K. 2011 Adsorption of chiral aromatic amino acids onto carboxymethyl-β-cyclodextrin bonded Fe_3O_4/SiO_2 core–shell nanoparticles. *Journal of Colloid and Interface Science* **354**(2), 483–492.

Giles, C., MacEwan, T., Nakhwa, S. & Smith, D. 1960 786. Studies in adsorption. Part XI. A system of classification of solution adsorption isotherms, and its use in diagnosis of adsorption mechanisms and in measurement of specific surface areas of solids. *Journal of the Chemical Society (Resumed)* **786**, 3973–3993.

Goscianska, J., Olejnik, A. & Pietrzak, R. 2014 Adsorption of l-phenylalanine on ordered mesoporous carbons prepared by hard template method. *Journal of the Taiwan Institute of Chemical Engineers* **45**(2), 347–353.

Hong, S. U. & Bruening, M. L. 2006 Separation of amino acid mixtures using multilayer polyelectrolyte nanofiltration membranes. *Journal of Membrane Science* **280**(1–2), 1–5.

Water Practice & Technology Vol 15 No 4
doi: 10.2166/wpt.2020.089

Jonckheere, D., Steele, J. A., Claes, B., Bueken, B., Claes, L., Lagrain, B., Roeffaers, M. B. & De Vos, D. E. 2017 Adsorption and separation of aromatic amino acids from aqueous solutions using metal–organic frameworks. *ACS Applied Materials & Interfaces* **9**(35), 30064–30073.

Kamran, S. 2016 Study of the adsorption of L-phenylalanine, L-tryptophan, and L-tyrosine from aqueous samples by Fe_3O_4 modified magnetic nanoparticles with ionic liquid. *Biquarterly Iranian Journal of Analytical Chemistry* **3**(2), 105–115.

Konggidinata, M. I., Chao, B., Lian, Q., Subramaniam, R., Zappi, M. & Gang, D. D. 2017 Equilibrium, kinetic and thermodynamic studies for adsorption of BTEX onto Ordered Mesoporous Carbon (OMC). *Journal of Hazardous Materials* **336**, 249–259.

Kopecka, I., Pivokonsky, M., Pivokonska, L., Hnatukova, P. & Safarikova, J. 2014 Adsorption of peptides produced by cyanobacterium *Microcystis aeruginosa* onto granular activated carbon. *Carbon* **69**, 595–608.

Laksaci, H., Khelifi, A., Trari, M. & Addoun, A. 2017 Synthesis and characterization of microporous activated carbon from coffee grounds using potassium hydroxides. *Journal of Cleaner Production* **147**, 254–262.

Langmuir, I. 1918 The adsorption of gases on plane surfaces of glass, mica and platinum. *Journal of the American Chemical Society* **40**(9), 1361–1403.

Li, X.-F. & Mitch, W. A. 2018 *Drinking Water Disinfection Byproducts (DBPs) and Human Health Effects: Multidisciplinary Challenges and Opportunities*. ACS Publications, Washington, DC.

Muellner, M. G., Wagner, E. D., McCalla, K., Richardson, S. D., Woo, Y.-T. & Plewa, M. J. 2007 Haloacetonitriles vs. regulated haloacetic acids: are nitrogen-containing DBPs more toxic? *Environmental Science & Technology* **41**(2), 645–651.

Plewa, M. J., Wagner, E. D., Muellner, M. G., Hsu, K. M. & Richardson, S. D. 2008 Comparative mammalian cell toxicity of N-DBPs and C-DBPs. In: *Disinfection by-Products in Drinking Water: Occurrence, Formation, Health Effects, and Control*. (T. Karanfil, S. W. Krasner, P. Westerhoff & Y Xie, eds) American Chemical Society, Washington, DC, pp. 36–50.

Readi, O. K., Girones, M. & Nijmeijer, K. 2013 Separation of complex mixtures of amino acids for biorefinery applications using electrodialysis. *Journal of Membrane Science* **429**, 338–348.

Sharma, V. K., Zhao, J. & Hidaka, H. 2014 Mechanism of photocatalytic oxidation of amino acids: Hammett correlations. *Catalysis Today* **224**, 263–268.

Shim, Y., Rixey, W. & Chellam, S. 2008 Influence of sorption on removal of tryptophan and phenylalanine during nanofiltration. *Journal of Membrane Science* **323**(1), 99–104.

Tang, S., Kong, L., Ou, J., Liu, Y., Li, X. & Zou, H. 2006 Application of cross-linked β-cyclodextrin polymer for adsorption of aromatic amino acids. *Journal of Molecular Recognition: An Interdisciplinary Journal* **19**(1), 39–48.

Thurman, E. M. 2012 *Organic Geochemistry of Natural Waters*. Springer Science & Business Media, Dordrecht, the Netherlands.

Titus, E., Kalkar, A. K. & Gaikar, V. G. 2003 Equilibrium studies of adsorption of amino acids on NaZSM-5 zeolite. *Colloids and Surfaces A: Physicochemical and Engineering Aspects* **223**(1–3), 55–61.

Tran, H. N., You, S.-J., Hosseini-Bandegharaei, A. & Chao, H.-P. 2017 Mistakes and inconsistencies regarding adsorption of contaminants from aqueous solutions: a critical review. *Water Research* **120**, 88–116.

Tran, H. N., Lin, C.-C. & Chao, H.-P. 2018 Amino acids-intercalated Mg/Al layered double hydroxides as dual-electronic adsorbent for effective removal of cationic and oxyanionic metal ions. *Separation and Purification Technology* **192**, 36–45.

Vo, P. T., Ngo, H. H., Guo, W., Zhou, J. L., Nguyen, P. D., Listowski, A. & Wang, X. C. 2014 A mini-review on the impacts of climate change on wastewater reclamation and reuse. *Science of the Total Environment* **494**, 9–17.

Weber, W. J. & Morris, J. C. 1965 Kinetics of adsorption in columns of fluidized media. *Journal (Water Pollution Control Federation)* **37**, 425–443.

Wu, F.-C., Liu, B.-L., Wu, K.-T. & Tseng, R.-L. 2010 A new linear form analysis of Redlich–Peterson isotherm equation for the adsorptions of dyes. *Chemical Engineering Journal* **162**(1), 21–27.

Zhang, R., Wang, F., Chu, W., Fang, C., Wang, H., Hou, M., Xiao, R. & Ji, G. 2019 Microbial degradation of typical amino acids and its impact on the formation of trihalomethanes, haloacetonitriles and haloacetamides during chlor(am)ination. *Water Research* **159**, 55–64.